

See discussions, stats, and author profiles for this publication at: <https://www.researchgate.net/publication/11323090>

Coupled Modes of the Resonance Box of the Guitar

Article in *The Journal of the Acoustical Society of America* · June 2002

DOI: 10.1121/1.1470163 · Source: PubMed

CITATIONS

74

READS

11,457

3 authors:



María Jesús Elejabarrieta

University of Deusto

68 PUBLICATIONS 1,272 CITATIONS

[SEE PROFILE](#)



A. Ezcurra

Universidad Pública de Navarra

32 PUBLICATIONS 822 CITATIONS

[SEE PROFILE](#)



Carlos M Santamaria

Universidad del País Vasco / Euskal Herriko Unibertsitatea

98 PUBLICATIONS 1,500 CITATIONS

[SEE PROFILE](#)

Coupled modes of the resonance box of the guitar

M. J. Elejabarrieta^{a)}

Departamento de Física Aplicada II, Universidad del País Vasco, Apdo. 644-48080 Bilbao, Spain

A. Ezcurra^{b)}

Departamento de Física, Universidad Pública de Navarra, 31006 Pamplona, Spain

C. Santamaría

Departamento de Física Aplicada II, Universidad del País Vasco, Apdo. 644-48080 Bilbao, Spain

(Received 1 November 2001; revised 5 February 2002; accepted 16 February 2002)

Vibrations of the resonance box of the guitar have been studied by means of the modal analysis technique and the finite-element method. An expert craftsman constructed the guitar box with all the structures, internal and external, characteristic of a real instrument for the experimental measurements. The boundary conditions were chosen in order to clarify the soundboard–back interaction only via the internal air coupling. The numerical model allows one to study the influence of each component on the whole box, and the contribution of the modes of the components (wooden box and its parts, and air), to the coupled modes by calculating their participation factors. The coupled modes of the guitar box are discussed taking into account both the finite-element and modal analysis results. © 2002 Acoustical Society of America. [DOI: 10.1121/1.1470163]

PACS numbers: 43.75.Gh [ADP]

I. INTRODUCTION

The guitar is a complex mechanical system because its dynamic behavior is determined by the interaction of several components. The plucked strings radiate only a small amount of sound directly, but they excite the bridge and the top plate, which in turn transfer energy to the air cavity, ribs, and back plate. Sound is radiated efficiently by the vibrating plates and through the sound hole. In particular, two main distinguishable parts form the guitar box: the wood structure and the inside fluid. This paper is devoted to the experimental and numerical determination of the vibrational behavior of the guitar box and forms part of a more extensive study addressing the vibrational behavior of the guitar and its pieces.

Several experimental and computational techniques have been applied to this issue. Holography and laser interferometry have provided very accurate information about guitar-box resonances^{1–4} both in classic and acoustic guitars, but are devoted mainly to the soundboard alone. Regarding the complete resonance box, Richardson⁵ analyzed its modal parameters under free-boundary conditions by means of holographic measurements. Another two techniques, the finite-element method and the modal analysis technique, are quantitative and complementary, since their results can be compared. The modal analysis technique allows an approach to the sound produced by the instrument, since the vibrational analysis is carried out on the complete body of the guitar: structure and fluid. By contrast, this type of analysis is not able to study the influence of each part of the guitar on the complete instrument in a direct way, and must be applied together with other techniques; for example, numerical calculation by the finite-element method. This latter method has

become an important tool for studying the vibrational behavior of complex mechanical systems, such as musical instruments.^{5–8} In this sense, the dynamics of the guitar soundboard both in free- and fixed-boundary conditions has been studied. The modal analysis technique was applied by Marshall⁹ to determine the vibrational behavior of the violin. In the case of the guitar box, some studies have been published previously on electromechanical input–output measurements at several points of the soundboard and their correlation with acoustic efficiency,^{3,10,11} although the modal parameters of the system were not determined.

Here, we report the calculated low-frequency modes and natural frequencies of the resonance box (top plate, back side, ribs, edges, and blocks) starting on the dynamics of the fundamental components: the top and back plates. The neck was not included. The boundary conditions were chosen in order to make the soundboard–back interaction clear exclusively through the internal air. First, the behavior of the complete box was obtained in the absence of air starting from the soundboard and back plate. This numerical model allowed us to evaluate the influence of the constructing process of the top and back plates on the definitive instrument. Then, the air inside the cavity was taken into account and the coupled modes were calculated. This computer calculation permits, on the one hand, a quantitative study of the interaction between the fluid and the structure, and on the other, to assess the influence of the constructing process of the top and back plates on the dynamics of the instrument.

The numerical model corresponds in detail to a real guitar box, as designed and constructed by a skilled craftsman. The modal analysis technique has been applied to determine the natural frequencies, vibration modes, and quality factors of this resonance box, under equivalent boundary conditions. Finally, the numerical and experimental results have been compared and discussed.

^{a)}Present address: Departamento de Mecánica, Mondragon Unibertsitatea, 20500 Mondragon, Guipuzcoa, Spain.

^{b)}Electronic mail: aezcurra@unavarra.es

II. EXPERIMENTAL SETUP

A. The guitar box

The system under study was a guitar resonance box. On the one hand, it was constructed as a “real” system, and on the other, as a numerical model. The materials and the construction process were decided by a skilled luthier. The top plate was made of Canadian cedar and the thickness varied from point to point (2–2.7 mm). Some additional structures were provided to the plate. In particular, two bars were placed perpendicular to the grain, respectively, over and below the sound hole. The upper bar had a constant rectangular cross section. The lower bar also had a rectangular section, but its height was reduced linearly from the two ends to the center of the bar. Seven fan struts were arranged in the classic way, according to the *Torres* distribution and two symmetrical struts were placed on the lowest part of the plate. The bars and fan struts were made of spruce. The final mass of the soundboard with the whole set of internal structures was 165.2 g. The dynamics of the soundboard was previously analyzed in the successive stages of its construction.¹²

The back plate was made of Indian rosewood (thickness 2 mm) with one longitudinal and three transversal spruce bars added. The final mass was 281.0 g. The ribs were also made of Indian rosewood (thickness 1.7 mm) and their height increased linearly from 97 mm in the upper zone to 105 mm in the lower part. The top and back plates were joined to the ribs along their contour by means of the edges or *junquillos*, rectangular pieces of 3×10 mm. Two blocks were added, in the lower and upper zones, to avoid the strain of the box. The tail block had a uniform, nearly rectangular cross section of 10×50 mm. The upper block had a width of 60 mm, and its length increased linearly from 75 mm at the top plate to 90 mm at the back. Both edges and blocks were made of spruce. The final mass of the box was 853.0 g.

Among other possibilities, the finite-element method allows one to obtain the vibrational behavior corresponding to complex mechanical systems through a computational simulation that simplifies the continuous system into a discrete system. The data required are the geometric size and shape, the boundary conditions of the piece, and the characteristics of the materials: density, elastic tensor, and damping. Here, we attempted to achieve a numerical model of the guitar box with a high degree of accuracy as regards both the geometrical design and the material parameters. A partial model was previously used to study the soundboard dynamics along its construction process.¹³ It should thus allow us to study the effects of several parameters on the behavior of the soundboard, both alone and when forming part of the box.

The numerical model evolved following the real manufacturing process designed by the craftsman, by modifying its geometric characteristics, and by adding the internal structures, and became quantitatively more complex as the procedure progressed. Figure 1 shows two images of half of the mesh defined for the resonance box of the guitar. The top plate was modeled with second-order brick elements (6590 nodes and 956 elements). The back plate was modeled with second-order brick elements (7362 nodes and 1116 elements). The ribs were modeled with second-order sheet ele-

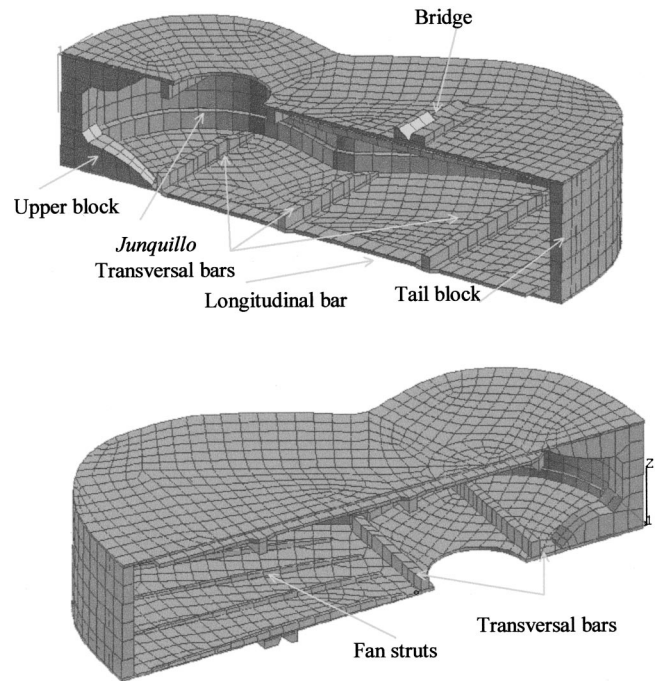


FIG. 1. Two longitudinal sections of the finite element mesh; the geometrical design and the added structures can be seen.

ments (1938 nodes and 612 elements). The bridge was modeled with first-order brick elements (116 nodes and 40 elements). The rest of the pieces, blocks and edges, were modeled with first-order brick elements, as were the bars and rods of the soundboard and back plate. The complete resonance box contained 15 946 nodes and 3132 elements. The resolution of the mesh guarantees the response up to 600 Hz.¹⁴ The material parameters used for the numerical model are shown in Table I. No viscous effects were considered, and hence the modes for both the independent domains and the coupled system were normal.

The mesh and the boundary conditions for the air inside the cavity have been described together with its dynamic behavior when the cavity is completely rigid in Ref. 15. The mesh had 8474 first-order cubic elements from the ABAQUS¹⁴ library, specific for acoustic media, and 10 788 nodes. The geometrical outline of the surface of the cavity included the internal struts. The values for the bulk modulus B and the density ρ of air are as follows: $B=142$ kPa and $\rho=1.2$ kgm⁻³, whereas viscous effects were not taken into account.

B. Numerical calculations

Regarding the numerical model, the analysis, and the interpretation of the results, the fluid–structure coupling is a

TABLE I. Elastic parameters and densities corresponding to the components of the guitar box as explained in the text.

Elastic constants	Canadian cedar	Indian rosewood	Spruce
E_1 (MPa)	5600	16 000	15 000
E_2 (MPa)	520	2 200	650
G_{12} (MPa)	600	1 100	600
ν_{12}	0.33	0.36	0.03
Density ρ (kg m ⁻³)	342	775	460

complex phenomenon. The coupling takes place at the interface of the two domains through the imposed boundary conditions. These domains describe different physical situations, but none of them can be analyzed without taking into account the influence of the others. In our case, the interaction was limited to small amplitude movements. The application of the finite-element analysis was accomplished using the ABAQUS software¹⁴ implemented on an Alpha 2100 workstation, in the case of the wooden box and the inner air individually. The coupled numerical model and application of the finite-element analysis were accomplished using the SYSNOISE software,¹⁶ since the ABAQUS software does not incorporate the algorithm of coupled modes analysis. On the other hand, SYSNOISE software only supports plate elements with homogeneous and isotropic materials, while ABAQUS has a wider element bookstore and options to describe different material behaviors, in particular orthotropic materials. Because coupling analysis and anisotropic materials were involved, both programs were necessary and all the information had to be transferred between them. Moreover, the data had to be adapted not only in their address format but also in their normalization factors. The results were renormalized from the previous unit amplitude normalization to modal mass unit by using the adequate normalization factors. After calculating the vibration modes of both the wooden box and the air, they were combined by means of the modal coupling method,¹⁶ which is based on the overlap and expansion of the vibration modes of the two uncoupled systems. Since the vibration modes of a system contain all the information about it, it is feasible to define such a system by its modal parameters (eigenvectors and eigenvalues) instead of defining it through its mechanical parameters (mass, stiffness, and damping). Regarding the boundary conditions, the ribs were considered as completely clamped to avoid their displacement, reproducing the experimental conditions of the modal analysis described afterwards.

Thus, the dynamic behavior of the resonance box of the guitar in the low-frequency range was calculated through the vibration modes of the structure and of the fluid inside the cavity, with the ribs fixed. On these uncoupled modes, the modal coupling method was applied to calculate the vibration patterns and natural frequencies of the coupled modes of the box. The interface is the air surface in contact with the inner surface of the box. Both surfaces are similar, but the nodes and elements do not coincide completely and hence the displacement of the structural nodes corresponding to the vibration modes of the air was interpolated on the nodes of the interface. Although several approximations are involved in the numerical method, the results are in fair agreement with the experimental measurements and allow us to analyze them.

C. Experimental measurements

The experimental method was the modal analysis technique.^{12,17} Among the available applications, the frequency response function (FRF) was chosen. The structure was put into vibration by a transducer hammer acting on successive points, and the response was recorded at one fixed point (the so-called roving hammer method) through an ac-

celerometer. More details can be found in Ref. 12. The frequencies studied were in the 0- to 800-Hz range, whereas the resolution was 1 Hz, although the estimation of the modal parameters was carried out in more reduced bands. Both the excitement and the response were perpendicular to the plates, the most important direction regarding the vibration and acoustic radiation of the final instrument. The response point was located at the position of the bridge, next to the bass string, and 230 excitation points were distributed over the soundboard (115) and the back (115). The number and location of the selected measurement points (maximum distance 5.85 cm; minimum distance 2.82 cm) covered the frequency range as well as the number of expected modes. The estimation of the modal parameters was global, since each modal analysis was made up of the 230 response functions. Therefore, the reported natural frequencies, the vibration modes, and the quality factors do not depend on the particular response point. The vibration modes obtained had a normal character with proportional viscous damping. The most relevant characteristics of the data acquisition and analysis can be found in Ref. 12. As for the boundary conditions, the ribs were fixed by means of polyurethane foam to a metallic mold, in order to prevent the soundboard and back-plate perimeters from moving in the analyzed frequency band.

III. RESULTS AND DISCUSSION

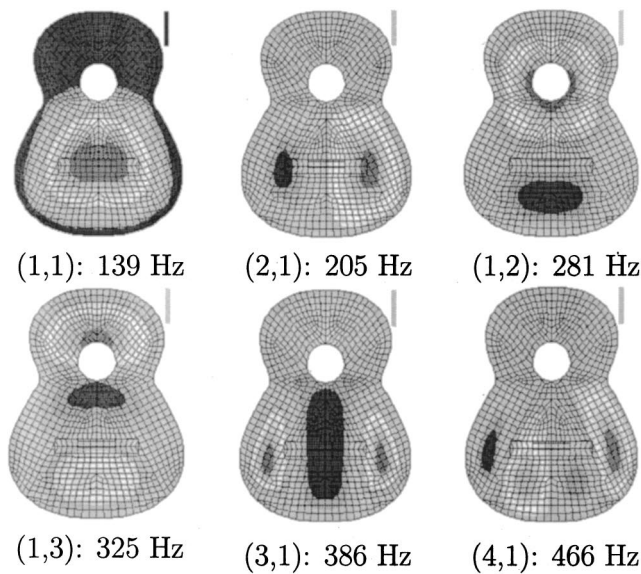
A. The soundboard and the back plate by the finite-element method

The starting point is the behavior of the main components of the box, soundboard and back plate, individually, under hinged boundary conditions; that is, allowing the edge to have zero displacement and free slope, the so-called simply supported boundary conditions. In this stage both components were finished with the complete strut system (bridge, transverse bars, and fan struts in the case of the soundboard, and longitudinal and transverse bars in the case of the back). Figure 2 shows the six lowest modes corresponding to each component, soundboard and back plate. The modes are named as (m,n) , m being the number of transverse half-waves and n the number of longitudinal half-waves on the plate,⁵ adding an "s" or a "b" to refer to the soundboard or to the back, respectively. As can be seen, the patterns are governed by the presence of the main struts. In the case of the soundboard, the position of the bridge determines the antinodal zones below the sound hole. In the case of the back, the transverse bars prevent the transversal flexure patterns from appearing in the low-frequency range and the antinodal zones are of small area and situated between the bar positions. Concerning the natural frequencies, the greater stiffness of the material of the back (rosewood), together with its stronger strut system, makes the frequency band broader in this component than in the soundboard.

B. The empty box by the finite-element method

In this section the eight lowest modes corresponding to the empty resonance box are presented. The soundboard and the back plate have now been attached to the ribs along with *junquillos* and blocks forming the "empty box;" that is,

Step s8p



Step b2p

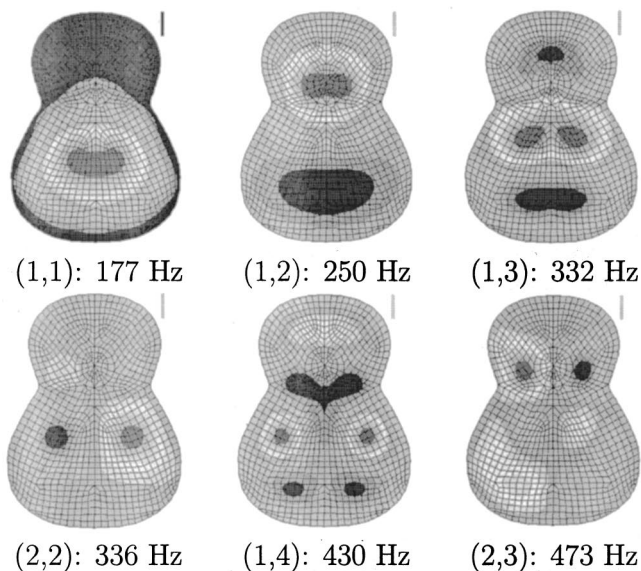


FIG. 2. Calculated modes of vibration and natural frequencies of the soundboard and the back in hinged boundary conditions. The stripe near each mode indicates the nodal zones color.

when the air is away. The patterns were normalized to unit amplitude, and were obtained by fixing the ribs; that is, imposing zero displacement and zero slope conditions. Each vibration mode is represented by two images, one corresponding to the soundboard and the other to the back plate. The two-dimension representation was chosen for clarity. Figure 3 shows the eight lowest modes of the empty resonance box. The frequency band is up to 500 Hz, covering more than half of the fundamental tones of the instrument. As can be seen, the vibration appears only in one part (soundboard or back) but not in both simultaneously. This result is obvious: if the ribs are fixed and the cavity is empty, there is no way to couple these two parts, and the modes are limited to only one of them. The names of the modes are as in the preceding stage, when the components were independent, although the shapes of some of them have changed.

If the soundboard and the back were identical both in design and material, two identical modes would appear at each natural frequency, one in each component. Not even in this case would coupling be present since there is no way of transmission, structural or acoustic, between the components. In our case, to a large extent the eight modes correspond to the vibration modes of the top (4) and back (4) plates with their contours fixed, although they are mainly affected by the blocks, the upper block (due to its size and position) being the most influential one. In the case of the back, the present modes are the fundamental mode (1,1)*b*, the longitudinal flexion modes (1,2)*b* and (1,3)*b*, and the shear mode (2,2)*b*. In the case of the soundboard, the patterns are the fundamental mode (1,1)*s*, the transverse flexural modes (2,1)*s* and (3,1)*s*, and the longitudinal mode (1,2)*s*.

Figure 3 suggests that some remarks should be made.

- (i) The vibration area is slightly greater in the soundboard than in the back for the (1,1) mode, and is located in the lower zone below the sound hole while the upper zone remains motionless. The amplitudes are not comparable since each mode has been normalized to unit amplitude.
- (ii) The aspect of mode (1,2) is similar in both components in the lowest antinodal zone. In the case of the upper maximum, it is situated in the zone of the sound hole for the top plate, and expanded by the two transverse bars in the case of the back.
- (iii) Although mode (3,1)*s* resembles a (3,2)*s* mode, it comes from the (3,1) mode of the soundboard with the contour fixed. The central antinodal zone is split into two, one of them below the bridge and the other one over the zone of the sound hole.
- (iv) Mode (1,3)*b* presents a similar split; in this case it resembles a (2,3)*b* mode.
- (v) In the case of modes (2,1)*s* and (2,2)*b*, their aspect is similar to that of the individual components with their contours fixed.

Concerning the natural frequencies, the only significant changes appear in the modes affected by the assembly of the box. In this case the modes are more rigid, since their frequencies increase in comparison with the results of the preceding section. The frequencies most sensitive to the assembly procedure are those of the patterns of the back (1,2)*b* and (1,3)*b*, with a relative increase of 15% with respect to the preceding stage. In the case of the top plate, the modes sensitive to the assembly procedure, (1,2)*s* and (3,1)*s*, increase their frequencies by less than 7%.

In view of the above, it is possible to predict the behavior of the resonance box by observing the dynamics of the independent components under fixed boundary conditions. The only modes affected are those presenting vibration in the zone of the upper block. This piece hinders the movement in its zone and increases the frequencies of the affected modes.

C. The air inside the box by the finite-element method

As mentioned above, the vibration modes of the enclosed air have been determined in a previous paper.¹⁵ To

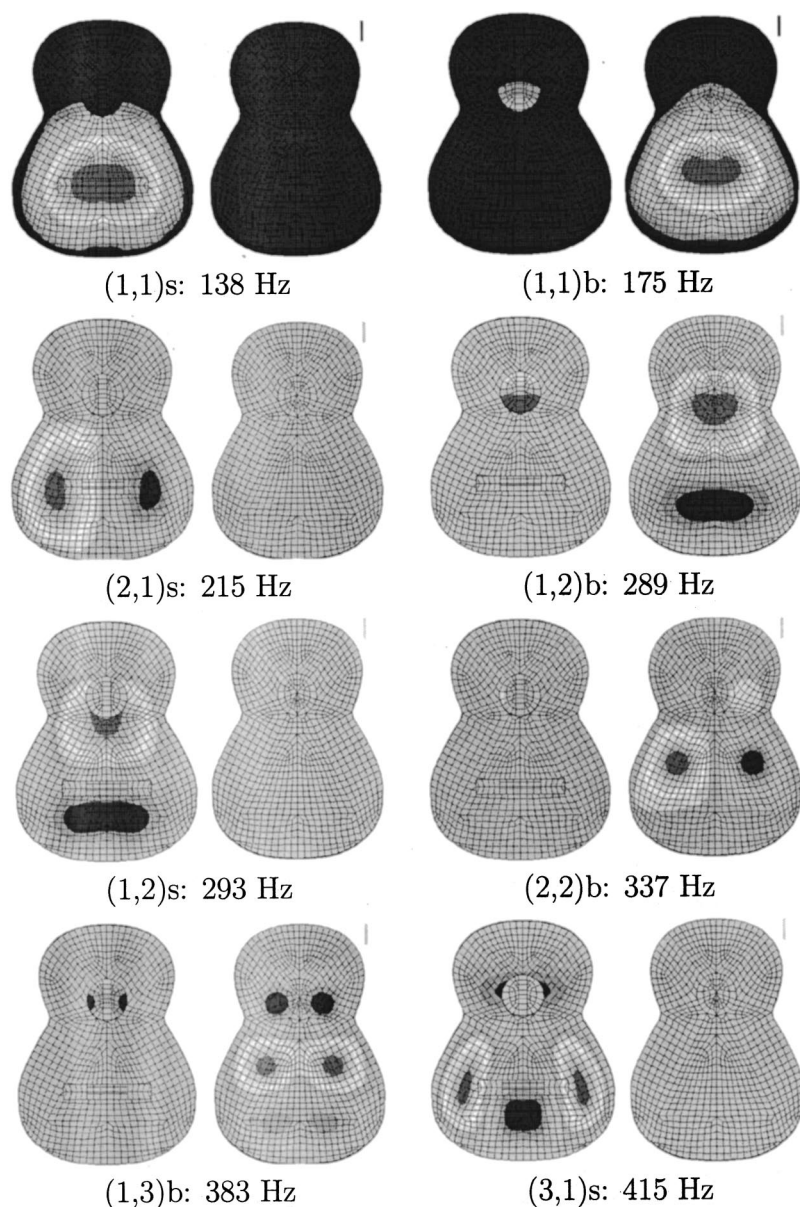


FIG. 3. Calculated modes of vibration and natural frequencies of the empty guitar box with the ribs fixed. The stripe near each mode indicates the nodal zones color.

resume, the fluid geometry corresponding to the guitar box, including internal bars and fan struts, was simulated. A preliminary finite-element model was used in order to define the boundary conditions on the sound hole so that the obtained internal modes were equal to those corresponding to the rigid box immersed in a much bigger space with free-boundary conditions on the external surfaces. The six lowest patterns were similar to those experimentally determined by other

authors.^{18–20} The calculated natural frequencies are presented in Table II, named in the usual way, starting from A0 (the so-called Helmholtz resonance).

D. The guitar box: Numerical calculations and experimental measurements

This section addresses the dynamics of the complete guitar box; that is, the coupled modes of the wood structure together with the inside air; these are indexed by the capital letters TB, referring to the top–back coupling, followed by the mode number, starting at the lowest frequency.

Figure 4 shows the eight lowest coupled modes, as determined by the finite-element method; since viscous effects were disregarded both in the wood structure and in the fluid, the coupled modes are normal. The boundary conditions were the same as in the preceding paragraph; that is, fixing the ribs. For graphic representation, the vibration amplitudes in both the soundboard and in the back show the coupled modes; for clarity's sake the additional struts have been

TABLE II. Natural frequencies of the air cavity of the guitar as determined by the finite-element method (Ref. 15).

Modes	Frequencies (Hz)
A0	155
A1	418
A2	545
A3	718
A4	771
A5	981

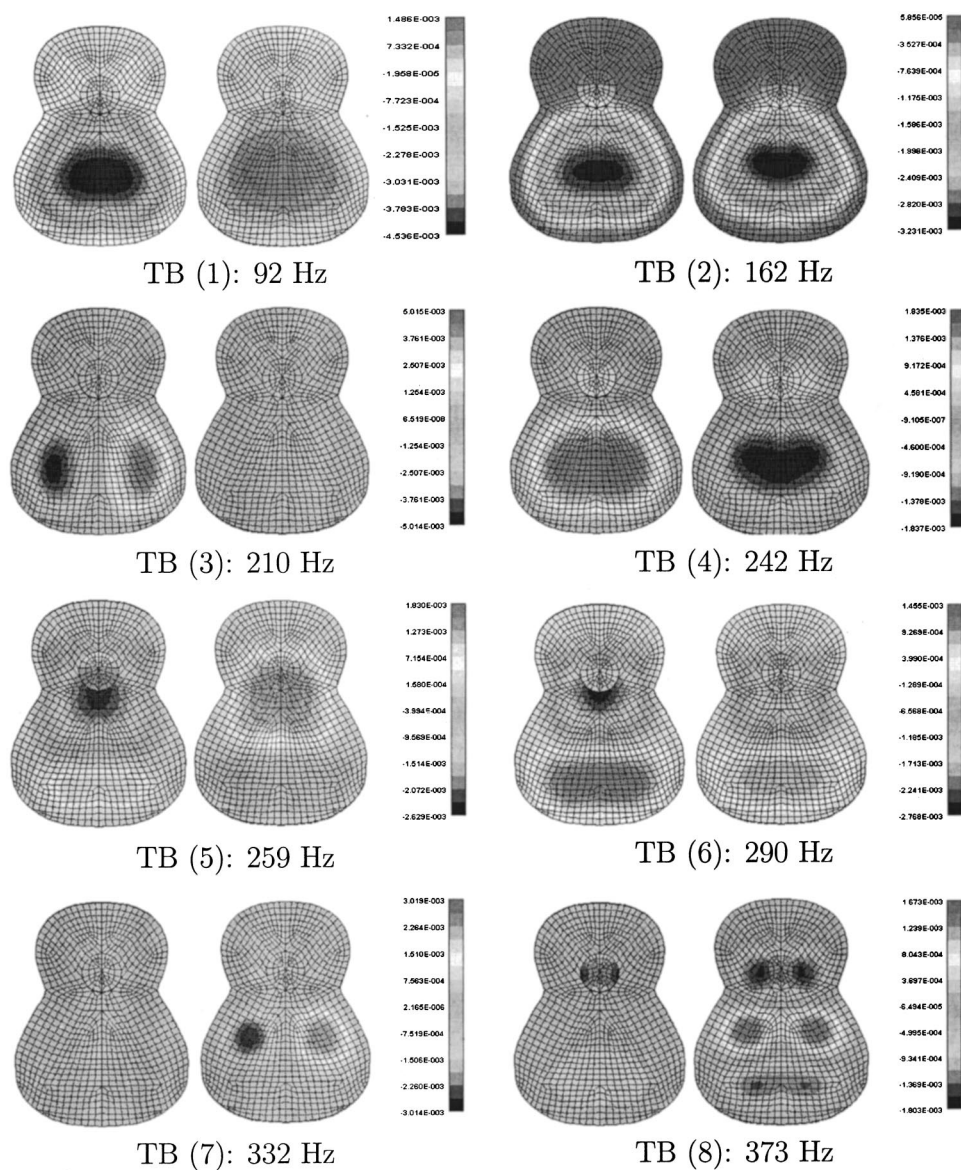


FIG. 4. Calculated coupled vibration modes and natural frequencies in (Hz) of the resonance box of the guitar with the ribs fixed. The back is viewed as if the soundboard were transparent. The colored stripe indicates the amplitude scale. The amplitude values cannot be compared with one another because they are independently normalized.

omitted in the figure, although they were taken into account in the whole analytical and experimental process. As can be seen, the air inside the cavity substantially affects the vibration patterns. Thus, it causes the soundboard and the back to move together at certain frequencies. Up to now both top and back plates had vibrated independently because there was no elastic medium for them to interact. The air contained in the box allows the connection between both structural components. In this way the coupling among the soundboard, the air, and the back gives rise to the modes of the box.

The calculated modes show that the influence of the air is greater at lower frequency. On comparing this figure with Fig. 3, it may be seen that the natural frequencies of the corresponding structural modes have decreased; this means that the fluid acts as an added mass. Moreover, the interaction between the structural and acoustic modes depends on the vibrational character of the structural modes. For example, some modes only appear in one component—top or back—i.e., the case of the transversal flexural modes.

Figure 5 shows the seven lower coupled modes, their eigenfrequencies and quality factors, as determined by the

modal analysis measurements. The vibration amplitudes are not comparable, since each pattern has been normalized to unit modal mass. The gray zones indicate immobility. Thus, from the figure it can be seen how the external edges of both the soundboard and the back remained fixed. This guarantees that the boundary conditions imposed on the ribs of the instrument prevent their movement and that the modes both in the soundboard and in the back are originated by the coupling of these structural components via the fluid of the cavity. Each vibration mode was estimated from the 230 responses of both plates. Because of this, each pattern in Fig. 5 represents the vibration in both components. Under these conditions, it is possible to compare the contour line density in the soundboard and in the back for each vibration mode. Thus, the number of contour lines in each component will be indicative of the amplitude of vibration in these structures. As can be seen, most of the largest amplitudes are situated in the lower and middle zones of the box in the analyzed frequency band.

As can be seen by comparing Figs. 4 and 5, the proposed finite-element model predictions are in fair agreement with

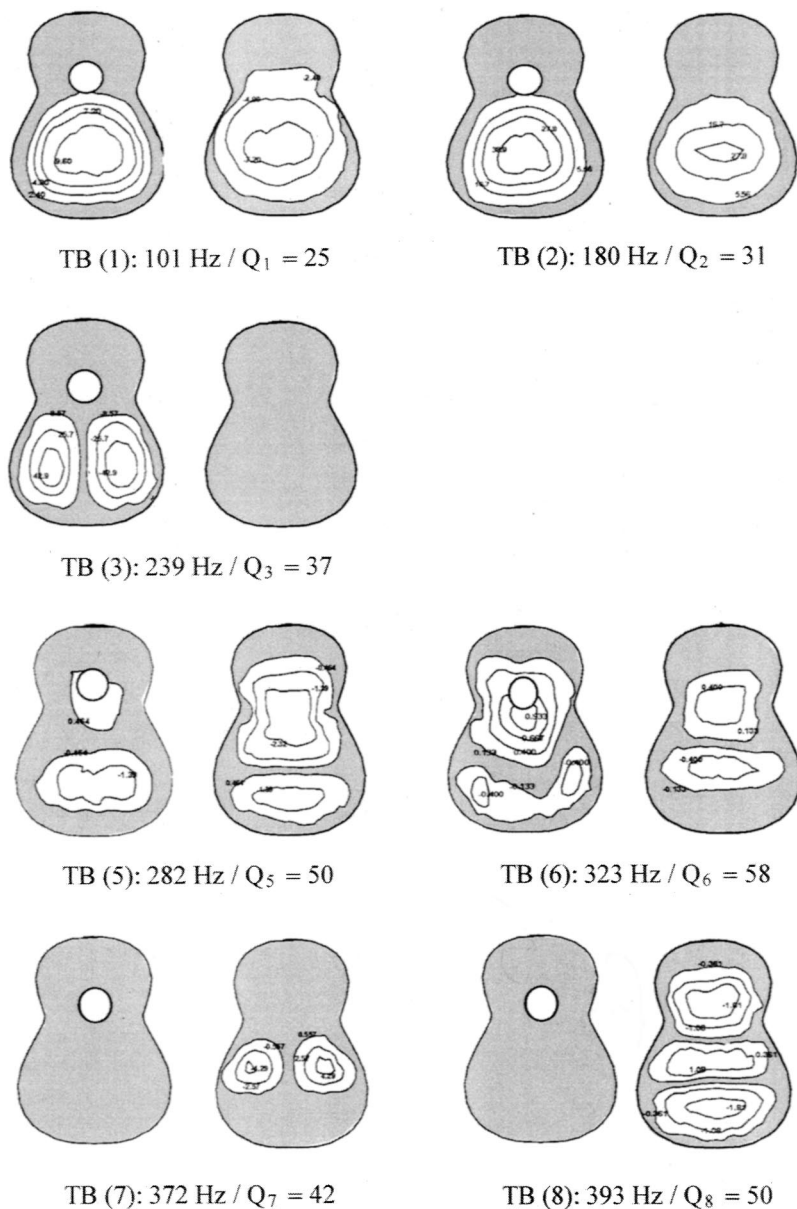


FIG. 5. Modes of vibration and natural frequencies of the resonance box of the guitar with the fixed ribs as obtained from experimental measurements analyzed by the modal analysis technique. The back is viewed as if the soundboard were transparent.

the experimental dynamics of the guitar box in the low-frequency range.

Figure 6 shows the modal participation factors of the uncoupled modes in the coupled modes. A pyramidal representation was adopted for the structural modes, and pie charts for the acoustic patterns. Furthermore, each mode is represented by a different fill pattern to facilitate identification. Contributions of less than 5% were disregarded. This participation index allows one to establish the origin of the coupled modes and to predict the necessary modifications in the soundboard and the back to obtain the desired effects on the definitive resonance box. The following sections are devoted to the analysis of the modes presented, accounting for the modal participation factors.

1. TB(1)

This is the fundamental mode of the resonance box. In this pattern the soundboard presents an antinodal zone at the position of the bridge. The upper zone of the soundboard

remains motionless due to the presence of the transverse bars and the upper block. Also in this case, vibration is limited to the lower part of the back but in this case the amplitude of vibration is three times smaller than in the soundboard in the calculated mode; the experimental results only indicate that the vibration amplitude is higher in the soundboard. Figures 4 and 5 show that the top-and back plates vibrate in phase opposition; this leads to considerable changes in the inner volume. Therefore, it is clear that the TB(1) mode is an efficient mode of radiation in the low-frequency band.²¹ TB(1) is originated from modes (1,1)*s* and (1,1)*b* of the empty resonance box (see Fig. 3), mainly interacting with the A0 air mode, as seen in Fig. 6. Mode A1 is also present, but its influence is negligible in comparison with the A0 mode. The principal structural mode is the soundboard's fundamental (1,1)*s*, with a participation factor of 70%. Thus, any modification to the soundboard, either the wood or the struts, would strongly affect the frequency and shape of this mode. In the case of the fluid, this mode is addressed by the Helm-

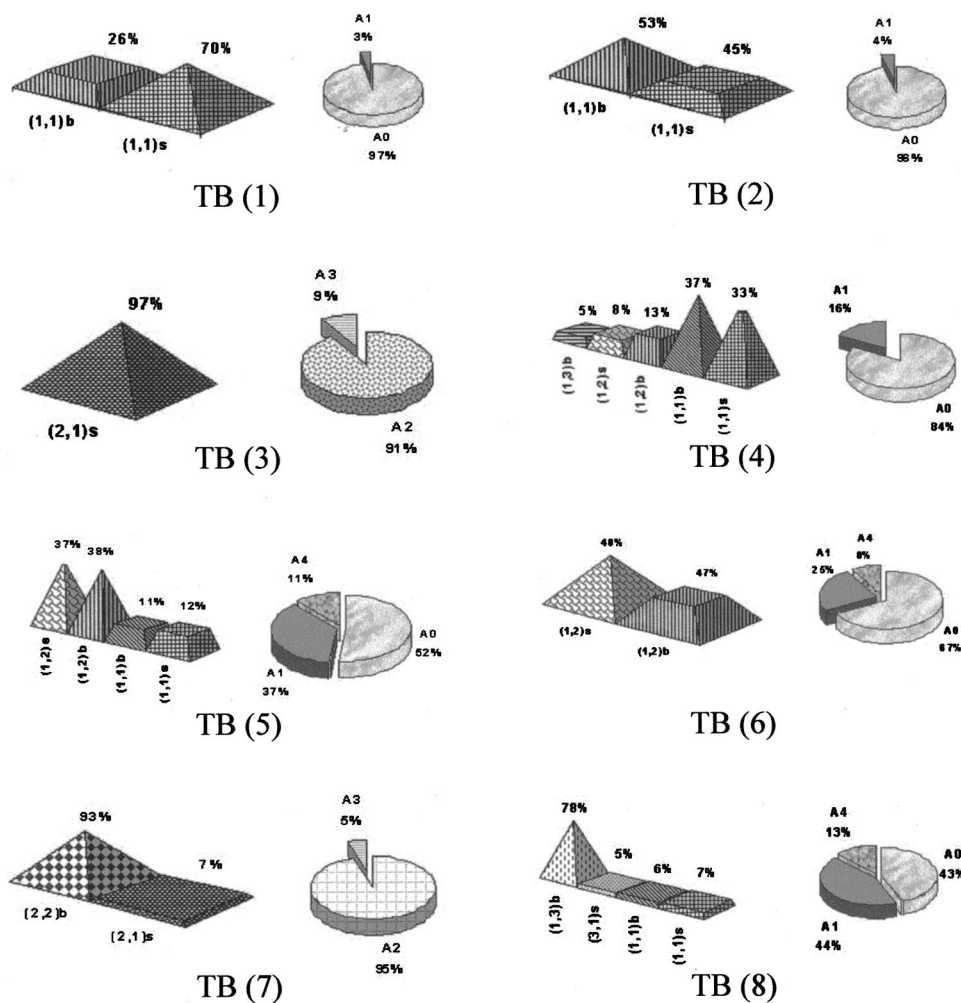


FIG. 6. Participation factors in (%) of the structural and acoustic vibration modes.

holtz resonance, and hence the height of the ribs or the size and shape of the sound hole would affect this fundamental mode of the resonance box. The frequency is reduced by 40% with respect to the empty box, pointing to the added mass effect of the fluid interacting with the structure.

2. TB(2)

The second vibration mode of the resonance box is named T(1,1) or first top plate resonance by other authors. The shape of this mode is similar to the TB(1) mode but in this case soundboard and back vibrate in phase, and so the involved volume changes in the inner air are smaller. Figure 5 shows that the maximum displacement of soundboard and back are equal and situated in the lower part of the box. Just as the TB(1) mode, this pattern is originated by the interaction of the fundamental modes of the soundboard $(1,1)_s$ and back $(1,1)_b$ with the Helmholtz mode A0. However, in contrast to mode TB(1), in this case the participation of the two modes of the empty box is nearly equal (see Fig. 6), hence, this mode will be equally sensitive to structural modifications in both the soundboard and the back plate. The $(1,1)_s - (1,1)_b$ coupling is mainly carried through the fundamental resonance of the air cavity A0, although mode A1 is also present. The frequency decrease with respect to the empty box highlights the added mass effect of the fluid, just as in the TB(1) mode. The importance of TB(2) has been

made clear by other authors, who have shown that it is the most efficient mode of radiation in the low-frequency band.^{3,21}

Both TB(1) and TB(2) have been analyzed by other authors^{19,21-24} experimentally and by means of simplified models. The theoretical models are able to justify the existence of these modes, but not to determine the proportions in which each component contributes to the coupling.

3. TB(3)

In this mode the back remains motionless: as has been explained before, the internal bars of the back hinder the vibration of its transversal flexural patterns and thus the contribution to radiation due to the back will be negligible. No changes were found on comparing TB(3) with $(2,1)_s$, either in pattern or in frequency, and therefore no soundboard-back coupling is present in this mode, so it can be analyzed as a soundboard mode. It will be sensitive, both in frequency and in the vibration amplitude, to the placement of the transversal bars and fan struts close to antinodal zones.¹³ The most influential acoustic mode is A2, for it presents a central longitudinal nodal line just like mode $(2,1)_s$.

4. TB(4)

Its pattern is similar to TB(1) mode, involving large volume changes, so TB(4) is an efficient mode of radiation, too.

It is originated from modes $(1,1)s$ and $(1,1)b$ of the empty box, mainly interacting with the A0 air mode. As the participation factors are similar to TB(1), the same considerations on the influence of the soundboard and the geometry of the cavity can be made in this case. Attending to this behavior, we can infer that this mode forms the low-frequency triplet together with TB(1) and TB(2);^{25,26} the calculated TB(4) is more complex than the theoretically predicted mode as the structural modes $(1,2)b$, $(1,2)s$, and $(1,3)b$ are present too. This mode could not be experimentally determined, probably due to the proximity of TB(3).

5. TB(5)

The soundboard and the back vibrate in phase opposition, with a longitudinal flexion character. The maximum vibration amplitude occurs around the sound hole in both plates. The lower part of the box, below the bridge, displays a weak movement that is more visible in the soundboard. The experimental measurements indicate that the vibration amplitude is larger for the back than for the soundboard; this fact is not so clear in the calculated mode. On analyzing this pattern (see Fig. 6), some remarks are merited. Regarding the wood structure, the soundboard and back contribute to the same extent, both of them providing two modes. Furthermore, the main modal participation is due to modes $(1,2)s$ and $(1,2)b$ and is three times higher than the participation of the corresponding fundamental modes. This mode is therefore governed by the longitudinal patterns of the soundboard and back.¹³ It will be sensitive to any change in the soundboard fan and to the distribution and shape of the transverse bars of the back. Regarding the acoustic modes, three patterns appear: A0, A1, and A4. Although mode A0 is still predominant, as in TB(1) and TB(2), here A1 and A4 have a notable participation in the coupling: also in this case, the structural–acoustic coupling is present when the modes have the same vibrational character. The participation of modes A1 and A4 implies that mode TB(5) is governed by the stationary waves of the air cavity, and hence the internal shape of the resonance box will influence this mode both through the structural response and through the air cavity response. This mode, like TB(1) and TB(2), is a strong radiator¹⁹ and together with the TB(6) mode covers most of the fundamental notes and most of the second partials of the lowest notes of the instrument.

6. TB(6)

This pattern presents a character of longitudinal flexion, just like TB(5), but in this case the soundboard and back vibrate in phase, so the air volume changes are smaller. Figures 4 and 5 show that the maximum amplitude happens at the soundboard, around the sound hole. Unlike mode TB(5), this mode presents a notable movement around the bridge and will therefore be easily excited by the strings. Figure 6 shows the structural and acoustic modes forming this pattern. The two structural modes are the longitudinal patterns $(1,2)s$ and $(1,2)b$ of the empty box (see Fig. 3) in equal proportions. The acoustic modes are A0, A1, and A4, as in TB(5), although the influence of A0 is higher in TB(6). Regarding

the frequency (290 Hz), this is almost equal to the frequency of the structural modes of the empty box (289 and 293 Hz).

Modes TB(5) and TB(6) form a symmetrical–antisymmetrical pair, as do TB(1) and TB(2). Both modes vibrate with a longitudinal flexion character with two antinodal zones in the lower and middle zones of each component. The presence of vibration all around the sound hole indicates that both modes will be efficient in sound radiation.

7. TB(7)

In this mode the soundboard remains motionless, just as the back did in TB(4). Both TB(4) and TB(7) have a transversal flexural character. Unlike mode TB(4), in which no back modes were present, in TB(7) the soundboard mode $(2,1)s$ certainly appears (participation 7%; see Fig. 6), although no soundboard vibration is evident in Figs. 4 and 5. The acoustical modes are the A2 mode (95%) and A3 (5%). Just as in mode TB(4), the air modes are those with a (zero-pressure) nodal line along the longitudinal axis of the box. Since this mode appears only in the back without coupling with the soundboard, acting on the strings will not excite it and so it does not contribute to the sound radiation and quality of the guitar.

8. TB(8)

This mode has a longitudinal flexural character in the back, presenting an antinodal region between the transverse bars. The soundboard remains nearly motionless, except for a slight vibration in the lower zone, not visible in the experimental results. The analysis of the modal participation of the structural modes (see Fig. 6) reveals that the major contributor is mode $(1,3)b$, the participation of the rest of the modes being less than 10%. Regarding the acoustic modes, A0 and A1 participate in equal proportions, whereas A4 makes only a small contribution. Taking into account that the frequency of the $(1,3)b$ mode is nearly equal to the frequency of this mode—TB(8)—it is possible to infer the limited influence of the inside air on this modal parameter. Due to the slight vibration of the lower part of the soundboard, acting on the strings will excite this mode, although the strongest vibration will occur on the back.

IV. CONCLUSIONS

The finite-element and the modal analysis methods have been applied to the resonance box of a guitar with the purpose of analyzing its vibrational behavior. The numerical model was developed progressively, starting with the soundboard and back, then the assembled box and the inside air separately, and finally the whole box; that is, the wood structure and the air together. In this way, mode evolution can be tracked, establishing the influence of each component on the final box. Comparison of the modal patterns and frequencies with the modal analysis results corresponding to a real guitar box confirms the quality of the model. The newest feature is the successful development of the model to calculate and analyze the box–air coupling. In this sense we can conclude that

- (1) Taking the air into account is essential to describe the vibrational modes of the guitar box;
- (2) The soundboard–back coupling via the inside air is efficient in some cases, in which it generates modes of similar geometry, with in-phase or opposite phase vibrations;
- (3) This coupling is decisive for the three lowest modes;
- (4) Modes presenting a longitudinal flexural character in both the soundboard and back of the empty box are able to couple;
- (5) Modes presenting a transverse flexural character either in the soundboard or in the back of the empty box produce noncoupled modes; that is, only one component vibrates;
- (6) The Helmholtz resonance participates whenever soundboard and back couple;
- (7) The influence of the inside air is decisive for the natural frequencies of the lowest modes of the box; and
- (8) The Helmholtz resonance is dominant for the two lowest modes, whereas the participations of A0 and A1 tend to be similar for the higher coupled modes.

ACKNOWLEDGMENTS

The authors are grateful to Keller, S.A., for their important collaboration, and very much obliged to Alberto Atxotegi, the craftsman, for his careful work.

- ¹E. V. Jansson, "A study of the acoustical and hologram interferometric measurements of the top plate vibrations of a guitar," *Acustica* **25**, 95–100 (1971).
- ²K. A. Stetson, "On modal coupling in string instrument bodies," *J. Guitar Acoust.* **3**, 23–29 (1981).
- ³I. M. Firth, "Physics of the guitar at the Helmholtz and first top-plate resonances," *J. Acoust. Soc. Am.* **61**, 588–593 (1977).
- ⁴R. R. Boullosa, "The use of transient excitation for guitar frequency response testing," *Catgut Acoust. Soc. Newsletter* **36**, 17–20 (1981).
- ⁵B. E. Richardson and G. W. Roberts, "The adjustment of mode frequencies in guitars: A study by means of holographic interferometry and finite element analysis," *SMAC'83*, Vol. II (Publication of the Royal Swedish Academy of Music, No. 46:2), pp. 285–302 (1985).
- ⁶H. L. Schwab, "Finite element analysis of a guitar soundboard I," *Catgut Acoust. Soc. Newsletter* **24**, 13–15 (1975).

- ⁷B. E. Richardson, G. W. Roberts, and G. P. Walker, "Numerical model of two violins plates," *J. Catgut Acoust. Soc.* **47**, 12–16 (1987).
- ⁸J. Bretos, C. Santamaria, and J. Alonso-Moral, "Vibrational patterns and frequency responses of the free plates and box of a violin obtained by finite element analysis," *J. Acoust. Soc. Am.* **105**, 1942–1950 (1999).
- ⁹K. D. Marshall, "Modal analysis of a violin," *J. Acoust. Soc. Am.* **77**, 695–709 (1985).
- ¹⁰G. W. Caldersmith, "Vibration geometry and radiation fields in acoustic guitars," *Acoust. Australia* **14**(2), 47–50 (1986).
- ¹¹J. C. S. Lai and M. A. Burgess, "Radiation efficiency of acoustic guitars," *J. Acoust. Soc. Am.* **88**, 1222–1227 (1990).
- ¹²M. J. Elejabarrieta, A. Ezcurra, and C. Santamaría, "Evolution of the vibrational behavior of a guitar soundboard along successive construction phases by means of the modal analysis technique," *J. Acoust. Soc. Am.* **108**, 369–378 (2000).
- ¹³M. J. Elejabarrieta, A. Ezcurra, and C. Santamaría, "Vibrational behavior of the guitar soundboard analyzed by the finite element method," *Acust. Acta Acust.* **87**, 128–136 (2001).
- ¹⁴ABAQUS (version 5.6), Hibbit, Karlsson, and Sorensen (1998).
- ¹⁵M. J. Elejabarrieta, A. Ezcurra, and C. Santamaría, "Air cavity modes in the resonance box of the guitar: the effect of the sound hole," *J. Sound Vib.* (in press).
- ¹⁶SYSNOISE, Lms, Belgium (1994).
- ¹⁷D. J. Ewins, *Modal Testing: Theory and Practice* (Research Studies, Taunton, Somerset, England, 1984).
- ¹⁸E. V. Jansson, "Acoustical properties of complex cavities and measurements of resonance properties of violin-shaped and guitar-shaped cavities," *Acustica* **37**(4), 211–221 (1977).
- ¹⁹T. D. Rossing, J. Popp, and D. Polstein, "Acoustical response of guitars," *SMAC'83*, Vol. II (Publication of the Royal Swedish Academy of Music, No. 46:2), pp. 311–332 (1985).
- ²⁰A. Runnemalm and N. E. Molin, "Air cavity modes in sound boxes recorded by TV holography," *Proceedings of the 2nd Convention of the European Acoustics Association: Forum Acusticum*, Berlin (1999).
- ²¹B. E. Richardson, "The acoustical development of the guitar," *Catgut Acoust. Soc. J.* **2**(5) (Series II), 1–10 (1994).
- ²²G. Caldersmith, "Plate fundamental coupling and its musical importance," *Catgut Acoust. Soc. Newsletter* **36**, 21–27 (1981).
- ²³O. Christensen and B. B. Vistisen, "Simple model for low-frequency guitar function," *J. Acoust. Soc. Am.* **68**, 758–766 (1980).
- ²⁴F. T. Dickens, "Analysis of the first and second vibration modes in a guitar using an equivalent electrical circuit," *Catgut Acoust. Soc. Newsletter* **35**, 18–21 (1981).
- ²⁵N. H. Fletcher and T. D. Rossing, *The Physics of Musical Instruments* (Springer, New York, 1991).
- ²⁶O. Christensen, "Qualitative models for low frequency guitar function," *J. Guitar Acoust.* **6**, 10–25 (1982).